Dynamical phase transitions in a parametrically modulated radio-frequency laser

R. Stoop
Physik-Institut der Universität Zürich-Irchel, CH-8057 Zürich, Switzerland

J. Parisi
Physikalisches Institut der Universität Tübingen, D-7400 Tübingen, Federal Republic of Germany and Physikalisches Institut der Universität Bayreuth, D-8580 Bayreuth, Federal Republic of Germany

(Received 4 June 1990)

In this contribution, we discuss dynamical phase-transition-like behavior in dynamical systems and give evidence for the occurrence of such effects in an experimental, parametrically modulated radio-frequency laser. We elucidate the connection between a generalized scaling behavior that depends on two scaling exponents, i.e., the fractal dimensions and the Lyapunov exponents, and the procedures available for the evaluation of scaling functions of Lyapunov exponents from experimental data.

I. INTRODUCTION

The scaling behavior of experimental dynamical systems has become a wide-ranging field of research since it was realized that for a description of such a system various mutually independent characterizations are necessary. The most prominent among these characterizations are the fractal dimensions and the Lyapunov exponents, on the one hand, and the different concepts of entropy and complexity, on the other hand. For a convenient description of a system, fluctuations of at least the first two quantities should also be taken into account. This is achieved by considering scaling functions of fractal dimensions and Lyapunov exponents.

In this contribution, we concentrate on the Lyapunov exponents and their scaling functions. We show that in the dynamical scaling behavior of NMR-laser data different phase-transition-like behaviors can be observed that indicate the usefulness of the thermodynamic approach to dynamical systems. A mathematical description of an appropriate dynamical system starts with the definition of a suitable generating partition. For a given system, many diverse generating partitions are possible, in principle, depending on the point of view one is interested in. If one wants to investigate the dynamical behavior, however, a partition is necessary that is "compatible" with the dynamical scaling behavior, i.e., a dynamical partition is required

II. THE PARTITION FUNCTION

Using such a partition consisting of M symbols, we proceed analogous to statistical mechanics and define the partition function for an attractor or repeller A (Ref. 1)

$$Z_G(q,\beta,n)=\sum_{j\in(1,\ldots,M)^n} l_j^{\beta}p_j^{q} \ . \tag{1}$$

Here the size of the jth region R_j of the partition is denoted by l_j, whereas the probability of falling into this region is denoted by p_j [$p_j=\int_{R_j}\rho(x)dx$, where $\rho(x)$ denotes the natural measure]. To account for the nonisotropy of the attractor, they can be thought of as vectors. β and q are sometimes called "filtering exponents." Local scaling of l and p in n (where n denotes the "level" of the partition) is expected. In this way, the length scale l and the probability p give rise to scaling exponents ε and α through

$$l_j=e^{-n\varepsilon_j} \ , \tag{2}$$

$$p_j=l_j^{\alpha_j} \ . \tag{3}$$

These exponents should be considered again as vectors. Using the above expression, from the partition function the generalized free energy F_G can be derived[2]

$$F_G(q,\beta)=\lim_{n\to\infty}\frac{1}{n}\ln\sum_{j\in(1,\ldots,M)^n} e^{-n\varepsilon_j(\alpha_j q+\beta)} \ . \tag{4}$$

A generalized entropy function $S_G(\alpha,\lambda)$ is then introduced through the global scaling assumption that the number of regions N which have scaling exponents between (α,ε) and $(\alpha+d\alpha,\varepsilon+d\varepsilon)$ scales as

$$N(\alpha,\varepsilon)d\alpha\,d\varepsilon\sim e^{S_G(\alpha,\varepsilon)}d\alpha\,d\varepsilon \ . \tag{5}$$

Writing the partition function formally as an integral, via a saddle-point approach, the relationship between the generalized free energy F_G and the generalized entropy S_G is found[2]

$$S_G(\alpha,\lambda)=F_G(q,\beta)+(\langle\alpha\rangle q+\beta)\langle\varepsilon\rangle \ , \tag{6}$$

where the angular brackets indicate that those values of α and ε leading to the maximum of Z_G (as a function of given q and β) have been chosen. In the following, we will omit the brackets. The free energy F_G or the generalized entropy S_G describe in this way the scaling behavior of the dynamical system. Note that the information-theoretical Renyi entropies evolve from (4) for $\beta=0$.

From the generalized free energy and entropy, respectively, two additional free energies and entropies can be derived by restriction: For $q=0$, we obtain the free energy first discussed by Oono and Takahashi[3(a)] as the maximum value of $S_G(\alpha,\varepsilon)$ with respect to variation of α alone for given ε. The associated free energy and entropy are in this case denoted by $F_G(\beta)$ and $S_G(\varepsilon)$, respectively. Similar approaches, which also correspond to a dynamical approach to the scaling behavior, have been put forward in Refs. 3(b)–3(f).

Furthermore, the fractal dimensions (see Refs. 4 and 5 and later, in a modified form, in Ref. 1) can also be obtained from $F_G(q,\beta)$ as the zeros $\beta_0(q)$ of $F_G(q,\beta)$ for given q.[6] The entropy-like function $f(\alpha)$ introduced in Ref. 1 (often called dimension spectrum) is then given by $S_G(\alpha_0,\varepsilon_0)=\varepsilon_0 f(\alpha_0)$, where ε_0 and α_0 lead to the zero of F_G for given q and appropriately chosen $\beta(q)$. From (6) it follows that $-\beta_0(q)=\alpha_0 q-f(\alpha_0)$. Due to the relationship with the fractal Hausdorff dimensions $D(q)$ $[-\beta_0=(q-1)D(q)]$, this point of view is often called the probabilistic approach. Note that in Ref. 1 $-\beta_0(q)$ has been denoted by $\tau(q)$. An analogous Legendre transformation relation can also be derived for the dynamical approach: It follows immediately from (6) that $S_G(\varepsilon)=\varepsilon\beta+F_G(\beta)$. This notation conforms to the pressure formalism used in Ref. 6. However, instead of $F_G(\beta)$, $-F_G(\beta)$ can also be used; the latter convention leads to the completely analogous Legendre transform situation if compared with the probabilistic approach.

III. MODEL SYSTEMS

For a simple example, let us recall the scaling behavior of the tent map

$$x \to x/l_1 \quad \text{for } x\in[0,l_1/(l_1+l_2)]\ ,$$

$$x \to (1-x)/l_2 \quad \text{for } x\in[l_2/(l_1+l_2),1]\ .$$

It is easy to see that for less than fully developed chaos and the fully developed case itself the fractal dimension is always equal to one [hence, the scaling function $f(\alpha)$ is trivial], while the Lyapunov exponents have a nontrivial scaling function. In the case of a strange repeller $(l_1+l_2<1)$, it can be shown that the scaling function of Lyapunov exponents and the scaling function of fractal dimensions are not mutually independent and can be derived from one another. The reason for this lies in the fact that the natural partition which is used is an equimeasure partition.

To account for more general situations, it has been proposed to include probabilities p_j as in (1) which cannot be expressed through the derivative of the dynamical map in such a simple way as, for example, for the tent map and other simple models.[6] Already for a three-scale Cantor set, a relatively complex scaling behavior is obtained which is shown in Figs. 1(a)–1(c). For a generic dynamical system which might be only asymptotically self-similar or might have no complete symbolic tree, the situation must be expected to be even more complicated.

As far as nonhyperbolic systems are concerned, in detail mainly maps of the interval or their two-dimensional analogs have been investigated. It has been found that for the exemplary family of maps $y=1-|1-2x|^z$ (Refs. 6 and 7) for $z=2$ an equimeasure partition can again be used; therefore, the probabilistic and the dynamical approach yield essentially the same scaling functions. A careful investigation of the free energy function in this nonhyperbolic case shows that, due to singularities in the natural measure, the free energy is no longer real analytic. This nonanalytic behavior can be interpreted as a phase transition (see also Sec. V). While for the above example the "temperature" at which this effect occurs is the same for both scaling functions, already the quartic map $(y=1-|1-2x|^4)$ shows that this needs not to be the case. For one-dimensional maps, the action of the dynamical partition can be described with the help of the generalized Frobenius-Perron operator;[8] for some of these maps, the natural measure then evolves as the eigenfunction of this operator for "temperature" $\beta=1$. It can, furthermore, be seen that (analogous to most "real" phase transitions) different eigenfunctions belong to different phases which can be characterized by different values of the temperature β.[9] In this way, they indicate the different symmetry or order properties of the different phases. For the dynamical and the probabilistic approach, phase-transition-like behavior has been detected in a number of prominent model cases, such as the Hénon map, the circle map, and the logistic map (Refs. 10, 11, and 6; see also Ref. 9). However, phase-transition-like behavior is not restricted to nonhyperbolic systems, as it can be shown to occur also for hyperbolic systems with more than one contracting direction.

IV. APPLICATION TO EXPERIMENTAL DATA

From the concept outline, it can be expected that phase-transition-like behavior could also be observed in experimental systems. For experimental data, it has been proposed in Ref. 6 to use the symbolic dynamics approach directly and to consider strings of symbols obtained from an experiment. This approach, however, is not as easy to follow as it seems, although interesting progress has been obtained for the Hénon and the Lozi maps in Ref. 12: There is no general recipe of how to obtain a generating partition, even for model systems.[13]

In the following, we therefore use a different formalism adapted to the generic situation of random sampling. We assume for the probabilistic approach that no distribution of length scales is known; for the dynamical approach, it is customary to sample in time. Accordingly, the scaling exponent ε is replaced by the Lyapunov exponent λ, and the scaling function $\phi(\lambda)$ corresponds to $S_G(\varepsilon)$. Note that for two-dimensional hyperbolic maps the two symbols denote identical quantities. As a consequence, instead of formula (4), the following set of relations emanates from (1). For the probabilistic approach,

$$\tau(q)=\lim_{\epsilon\to 0}\frac{\ln\langle P(B(x,\epsilon))^{q-1}\rangle}{\ln\epsilon}\ , \tag{7}$$

$$P(B(x,\epsilon))\sim\epsilon^{\alpha(x)}\ , \tag{8}$$

where $P(B(x,\epsilon))$ is the probability for a randomly

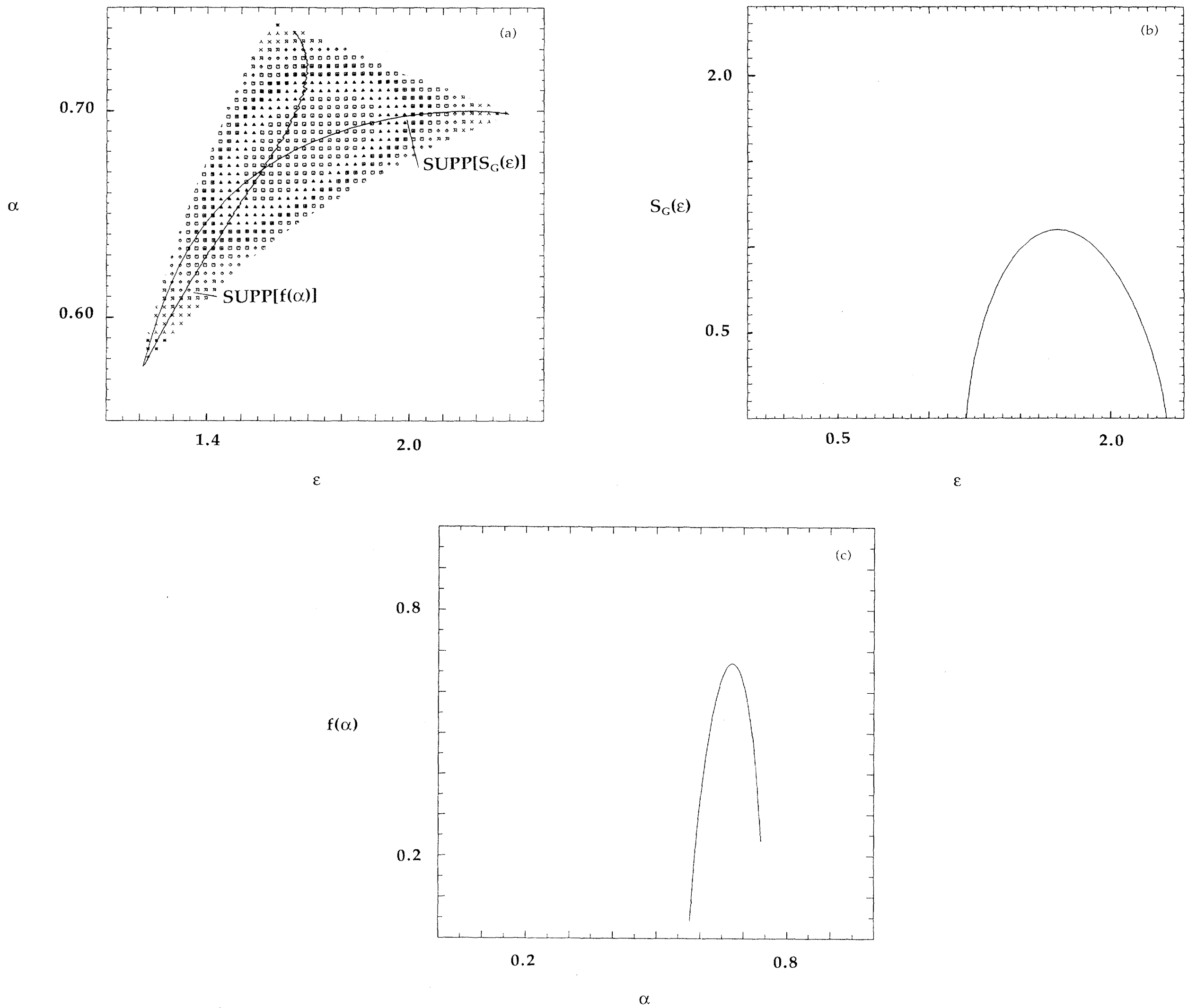

FIG. 1. Scaling behavior of the three-scale Cantor set. (a) α-ε area on which the entropy $S_G(\alpha,\varepsilon)$ is nonzero. The lines are indicated along which the functions $S_G(\varepsilon)$ and $f(\alpha)$ are evaluated. Different symbols indicate the different values of $S_G(\alpha,\varepsilon)$. However, more information can be obtained from (b). (b) $S_G(\varepsilon)$ for the three-scale Cantor set. The fact that the maximum is ln3 indicates the complete symbolic tree. (c) $f(\alpha)$ evaluated for the same model as in (a) and (b). Observe again the smooth shape of the graph (no phase-transition-like behavior).

chosen point of having a smaller distance than ϵ from point x,

$$f(\alpha)=\alpha q-\tau(q)\ , \tag{9}$$

$$\alpha(q)=\frac{d\tau(q)}{dq}\ , \tag{10}$$

$$P(\alpha,\epsilon)d\alpha\sim\epsilon^{\alpha-f(\alpha)}d\alpha\ . \tag{11}$$

For the dynamical approach,

$$\Lambda(\beta)=\lim_{n\to\infty}\frac{\ln\langle(DF_a^{n,+})^{-(\beta-1)}\rangle}{\ln\mathcal{T}}\ , \tag{12}$$

where $\mathcal{T}\equiv e^{-n}$, and $DF_a^{n,+}$ denotes the product of the stretching factors of absolute values larger than 1 in the tangent bundle associated with the n-times iterated dynamical map F_a,

$$P(x,\mathcal{T})\sim\mathcal{T}^{(1/n)\ln[DF_a^{n,+}(x)]}\ , \tag{13}$$

$$\phi(\lambda)=\beta\lambda-\Lambda(\beta)\ , \tag{14}$$

$$\lambda(\beta)=\frac{d\Lambda(\beta)}{d\beta}\ , \tag{15}$$

$$P(\lambda,k)d\lambda\sim e^{-k[-\phi(\lambda)+\lambda]}d\lambda \tag{16}$$

[note again that, in a strict sense, the interpretation of $P(x,\mathcal{T})$ as a probability holds only for the hyperbolic case].

V. THERMODYNAMIC FORMALISM

For each of the two approaches, a thermodynamic formalism can be formulated separately. As an example, we consider the dynamical approach. In the mapping onto a thermodynamic formalism[14] time is considered as a one-dimensional lattice. Negative lattice sites correspond to backward iteration, positive lattice sites to forward iteration in time. The partition function corresponding to Eq. (1) can be written as

$$Z_{c,s}(V,T)=e^{-F_s(V,T)/k_BT} = \sum_{S_n} e^{-n(\beta-1)\lambda(n,x_0)} \sim e^{-n(\beta-1)K(\beta)} \tag{17}$$

and is identified with a canonical ensemble. The microstates S_n are characterized by fixed volume and differing energies such that the following identification can be made (though not in a unique way):

$$E=(-n)\lambda \le 0, \quad 1/k_BT=-(\beta-1) ,$$

$$V=n>0, \quad F_s(V,T)=(-n)K(\beta) ,$$

where E denotes energy and k_B the Boltzmann constant.

The microcanonical description that deals with all ensembles with energies in the range $[E,E+dE]$ is associated with the partition function

$$Z(E,V)=e^{S(E,V)/k_B} \sim e^{(-n)[\lambda-\phi(\lambda)]} \tag{18}$$

which relates via the saddle-point approach to the functions ϕ and Λ, where now the nondifferentiable case is considered:

$$\Lambda(\beta)=\inf_\lambda[\beta\lambda-\phi(\lambda)], \tag{19}$$

$$\phi(\lambda)=\inf_\beta[\beta\lambda-\Lambda(\beta)] . \tag{20}$$

From the last two equations, it follows that

$$K(\beta)=\lambda(\beta)-\frac{\phi(\lambda)-\lambda}{\beta-1} \tag{21}$$

which can be interpreted as the classical thermodynamic relation

$$F_{s,v}(T)=E_v-TS_v , \tag{22}$$

where the subscript v is used to denote the original quantities divided by the volume. As can be checked, all thermodynamic relations follow. In particular, $(\partial S/\partial E)_V=1/T$ and $(\partial S/\partial V)_E=p/T$, where p denotes the pressure $[p=K(\beta)]$, ensure that this set can be taken as an axiomatic thermodynamic system. By using the analogy between the scaling of the support and the scaling of the measure, a corresponding interpretation can be given for the scaling of the measure (with $-n$ replaced by $\ln\epsilon$). In both cases, the corresponding entropy S is a convex function of E and V, E is convex in S and V, etc. From that property of S, it follows that a point on the graph of S is either extreme or an inner point of a linear part of it. The former can be identified with pure phases, the latter with mixtures, since points of nonanalytic behavior of $\Lambda(\beta)$ [$\tau(q)$, respectively] will lead to such parts of S. They are responsible for a phase-transition-like behavior of the system.

In view of the generalized case where two scaling indices are present, such a close analogy to the thermodynamic formalism is not possible (however, the ensemble could be viewed as an isobar-isotherm ensemble).[15] The simplest example of a phase-transition-like behavior in both the probabilistic and the present dynamical approach is provided by the coexistence of a repeller and an attractor. More specifically, it has been pointed out that phase-transition-like effects are to be expected generically from the existence of homoclinic tangency points.[16,17,7] Qualitatively different effects are obtained from systems at a crisis.[18,19] In Fig. 2 a schematic picture of the two cases is shown.

VI. EXPERIMENTAL RESULTS FROM THE NMR LASER

The ruby NMR laser[20] is one of the ideal systems for an experimental application since it possesses a variety of nonlinear behaviors. This behavior results from a strong nonlinear reaction to weak external modulation of parameters at low frequencies ($\sim$100 kHz). Upon alteration of the modulation amplitude A (experimentally, in most cases the quality factor of the resonator cavity was modulated, but other possibilities also exist), the most prominent features that can be observed are bifurcations of different types and crisis. The latter is triggered by a collision between attractors and unstable trajectories. For low modulation amplitudes, the NMR laser can be described in a satisfactory way by Lorentz-type equations

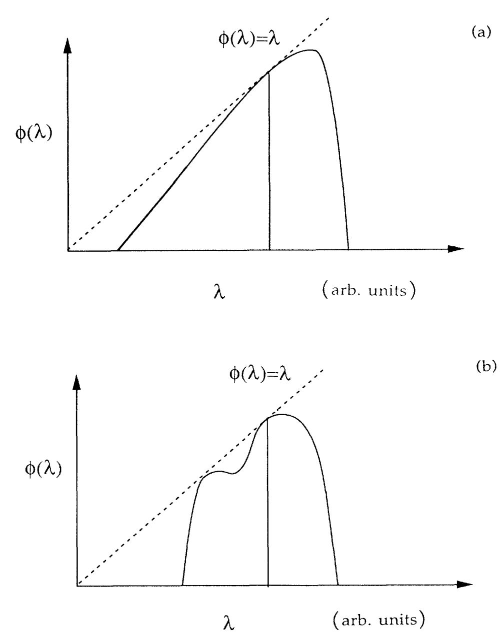

FIG. 2. (a) Schematic drawing of a phase-transition-like effect caused by the coexistence of a repelling fixed point A and an attractor B for the dynamical function $\phi(\lambda)$. (b) Schematic drawing of the scaling function $\phi(\lambda)$ in presence of a crisis.

derived from the Bloch-Kirchhoff equations. Due to necessary adiabatic elimination, in order to achieve chaotic behavior, the phase space has to be enlarged by parametric modulation. Let us point out, however, that for higher modulation amplitudes the system shows fractal dimensions larger than three and more than one positive Lyapunov exponent. Using a term coined by Roessler,[21] the latter states can be called hyperchaotic. In this case, the former set of equations is no longer sufficient, and for a description of the system other transitions than the spin $1/2 \rightarrow -1/2$ transition have to be taken into account.

In the following, we present the scaling functions of the Lyapunov exponents for two exemplary experimental files taken at different small modulation amplitudes A (see Fig. 3). From data files of at least 250 000 integers taken with 12-bit resolution, the Lyapunov exponents have been calculated, and the scaling functions have been derived. For the numerical evaluation, the algorithm described in Refs. 3(f) and 22 has been used. The first file was recorded at the modulation amplitude $A \sim 0.40$, whereas the second situation occurred for $A \sim 0.48$ (for experimental details, see Ref. 20). When the modulation amplitude is smoothly changed from the first value to the second, before the second value is reached a crisis sets in. There, the attractor abruptly changes its shape, and a larger area of the phase space is occupied in comparison to the situation before. Furthermore, a much more irregular behavior is displayed. On one hand, this qualitative change is indicated by an increase of the information dimension from about 2.2 to 2.8. But also the spectrum of Lyapunov exponents changes considerably; after the crisis, the first exponent becomes more than twice as large if compared to the old value. With reference to the theoretical outline given above, the scaling functions of the Lyapunov exponents for the two situations [Figs. 3(a) and 3(b)] are of interest. In particular, we focus on two facts.

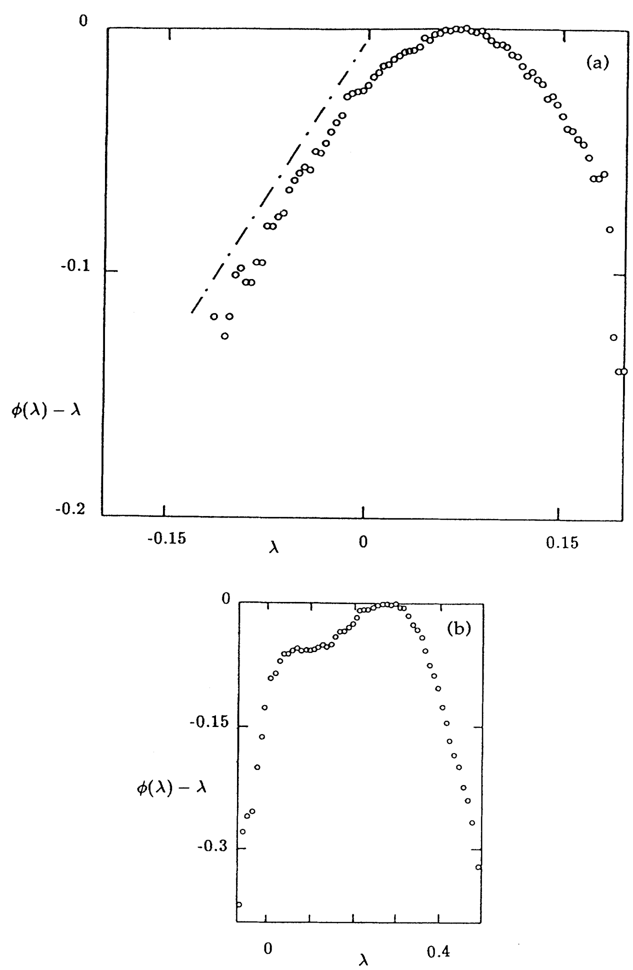

FIG. 3. (a) Phase-transition-like effect for the dynamical scaling function $\phi(\lambda)$ for the experimental NMR laser, far away from a crisis, due to the presence of homoclinic tangency points. (b) Phase-transition-like effect for the dynamical scaling function $\phi(\lambda)$ for the experimental NMR laser due to the presence of a crisis.

For the first file, we note a straight-line behavior on the left-hand side of the scaling function [Fig. 3(a)]. This behavior is believed to be due to the presence of homoclinic tangency points. From theoretical considerations for a dynamical map with a quadratic maximum, a line of slope 1 would be expected.[19] Our numerical investigations yield a slope which is somewhat larger. Taking into account the accuracy of the methods used, such an interpretation, however, is not inconsistent: It has been observed, when comparing scaling functions obtained from dynamical equations with scaling functions from time series of the same model that for the scaling functions from time series the left-hand slope is overestimated. This effect is probably due to a "smearing" of the homoclinic tangency points, which are responsible for the most negative Lyapunov exponents, by the discretization and the embedding processes. As a second element, the finiteness of the data could account for such a deviation.

In the scaling function of the second file [see Fig. 3(b)], a two-humped structure is evident. This item can be seen as the information contained in the scaling function about the crisis that has occurred before. The first hump of the scaling function is characteristic for the remainder of a merged attractor after an attractor-merging crisis. The situation should be compared with the results obtained in Ref. 19, where the same effect was found and discussed for the circle map. The scaling function obtained from this model system is almost identical with the scaling function of the NMR laser after the crisis.

Let us point out that at a higher modulation amplitude far from crisis where the NMR laser displays hyperchaotic behavior, again a scaling function of the form as reported in Fig. 3(a) is obtained. For this case, note that the fluctuation of the sum of the positive Lyapunov exponents has to be considered [see also Ref. 3(f)].

VII. CONCLUSION

Theoretically predicted phase transitions could be detected from experimental NMR-laser files. In this way, it is indicated that calculated scaling functions are a powerful means for the characterization of experimental data. For example, visual observation of a crisis has been corroborated with the help of the calculated scaling function and by comparison with the behavior of a well-known model system. Proceeding this way, one might be led to new insights into experimental systems. As far as the phase-transition-like behavior is concerned, we note, however, that the above observed phase transitions should not be interpreted as phase transitions with respect to the generalized formalism [i.e., with respect to $S_G(\alpha,\varepsilon)$], but rather with respect to the more specific scaling function $\phi(\lambda)$. In order to establish a more explicit connection between these two functions than presented here, more model cases should be investigated from this point of view.

ACKNOWLEDGMENTS

We acknowledge interesting discussions with E. Schoell, E. Brun, R. Holzner, and J. Peinke. We profited from generous communications with T. Tél. We thank the NMR-laser group of the Zürich University for providing us with the experimental data.

---

[1] T. C. Halsey, M. H. Jensen, L. P. Kadanoff, I. Procaccia, and B. Shraiman, Phys. Rev. A **33**, 1141 (1986).

[2] M. Kohmoto, Phys. Rev. A **37**, 1345 (1988).

[3] (a) Y. Oono and Y. Takahashi, Prog. Theor. Phys. **63**, 1804 (1980); (b) J. P. Eckmann and I. Procaccia, Phys. Rev. A **34**, 659 (1986); (c) M. Sano, S. Sato, and Y. Sawada, Prog. Theor. Phys. **76**, 945 (1986); (d) P. Szepfalusy and T. Tél, Phys. Rev. A **34**, 2520 (1986); (e) T. Horita, H. Hata, H. Mori, T. Morita, and K. Tomita, Prog. Theor. Phys. **80**, 923 (1988); (f) R. Stoop, J. Peinke, J. Parisi, B. Roehricht, and R. P. Huebener, Physica D **35**, 425 (1989).

[4] A. Renyi, *Probability Theory* (North-Holland, Amsterdam, 1970).

[5] P. Grassberger and I. Procaccia, Physica D **13**, 34 (1984).

[6] T. Bohr and D. Rand, Physica D **25**, 387 (1987).

[7] T. Bohr and T. Tél, in *Directions in Chaos,* edited by Hao Bai-Lin, (World Scientific, Singapore, 1988), Vol. II, p. 194.

[8] P. Szepfalusy, T. Tél, A. Csordas, and Z. Kovacs, Phys. Rev. A **36**, 3525 (1987).

[9] M. J. Feigenbaum, I. Procaccia, and T. Tél, Phys. Rev. A **39**, 5359 (1989).

[10] P. Grassberger (unpublished).

[11] P. Cvitanovic (unpublished).

[12] P. Cvitanovic, G. Gunaratne, and I. Procaccia, Phys. Rev. A **38**, 1503 (1988).

[13] P. Grassberger and H. Kantz, Phys. Lett. **113A**, 235 (1985).

[14] Ya. G. Sinai, Russ. Math. Surv. **27**, 21 (1972); D. Ruelle, *Thermodynamic Formalism* (Addison-Wesley, Reading, MA, 1978).

[15] T. Tél, Z. Naturforsch. **43a**, 1154 (1988).

[16] S. Newhouse, *Dynamical Systems* (Birkhaeuser, Boston, 1980).

[17] J. Guckenheimer and P. Holmes, *Nonlinear Oscillations, Dynamical Systems and Bifurcations of Vector Fields* (Springer, New York, 1986).

[18] C. Grebogi, E. Ott, and J. A. Yorke, Phys. Rev. Lett. **48**, 1507 (1982).

[19] T. Horita, H. Hata, H. Mori, T. Morita, S. Kuroki, and H. Okamoto, Prog. Theor. Phys. **80**, 809 (1988).

[20] P. Boesiger, E. Brun, and D. Meier, Phys. Rev. Lett. **38**, 602 (1977).

[21] O. E. Roessler, Phys. Lett. **71A**, 155 (1979).

[22] R. Stoop and P. F. Meier, J. Opt. Soc. Am. B **5**, 1037 (1988); R. Stoop and J. Parisi, Physica D (to be published).